THE SYNTHESIS OF RIBOSOMES IN *E. COLI*

III. SYNTHESIS OF RIBOSOMAL RNA

B. J. MCCARTHY, R. J. BRITTEN, *and* R. B. ROBERTS

From the Carnegie Institution of Washington, Department of Terrestrial Magnetism, Washington, D. C.

ABSTRACT Techniques of chromatography on columns of DEAE[1] cellulose and sedimentation analysis through a sucrose gradient have been used to study the flow of C^{14}-uracil label through precursors to completed ribosomes. Analysis by chromatography shows the existence of two sequential precursors constituting together some 10 per cent of the total ribosomal RNA. The chromatographic separation into three fractions is ascribed to the lower protein/RNA ratios of the precursor. By sedimentation the primary precursor (eosome) is identified as a component of average sedimentation coefficient 14S. The second precursor stage (neosome) is divided among at least two particles, one of 43S and the other of about 30S. Detailed kinetic analysis shows that all the radioactivity passes through the eosome on its way to finished 50S and 30S ribosomes. The delay in the entry of radioactivity to ribosomes is that expected from the quantity of eosome precursor. The obvious conclusion that there exists a precursor-product relationship is discussed together with possible interpretations.

A. INTRODUCTION

A number of experiments have shown that ribosomes serve as the principal sites of protein synthesis in living cells (McQuillen, Roberts and Britten, 1959). In addition, ribosomes are an essential ingredient for the low but probably significant rate of peptide bond synthesis which occurs in cell-free systems (Tissières *et al.*, 1960). In the larger cells, the ribosomes appear capable of protein synthesis in regions remote from DNA. Thus the information needed to arrange the amino acids in proper order must reside in the material of the ribosome or in a part of that material. Accordingly, a study of the biosynthesis of ribosomes might reveal not only the assembly of an important part of the cells' synthetic machinery but also indicate the mechanism by which the information of the DNA directs the synthesis of specific proteins.

Our studies of ribosome synthesis have continued since 1957. Progress in our understanding of the process has been reported annually (Roberts *et al.*, 1958,

[1] DEAE= diethylaminoethyl

1959, 1960) and at various meetings (Roberts, 1960). In addition some particular aspects of the work have been published (Roberts, Britten, and Bolton, 1958; McCarthy and Aronson, 1961). The earliest work (Roberts *et al.*, 1958) showed clearly that tracer material, en route to mature ribosomes, passed through several precursor stages. These were distinguished by differences in their chromatography and in their sedimentation. In 1958 it was estimated that roughly 10 per cent of the RNA was found in the precursor stage as nucleic acid or nucleoprotein of low protein content.

Several changes in technique have recently been introduced which make significant improvements in the accuracy of the measurements and in the possibility of interpretation. In the early experiments there was some degradation of ribosomes during chromatography on DEAE cellulose. This degraded material contaminated the precursor region and obscured the kinetics. This difficulty has been reduced by the use of a higher magnesium concentration in the eluting fluid. The accuracy of the measurements has been improved throughout by using P^{32} as a measure of total RNA together with C^{14}-uracil to indicate newly formed RNA.

This technique also permits the use of much smaller quantities of material so that much higher resolution can be obtained in sedimentation analysis. In particular, sedimentation analysis carried out in low concentrations of magnesium (10^{-4} M) has greatly aided the interpretation of all the results. Under these conditions two precursor stages are separable from the product material. In high magnesium concentrations the first precursor is associated with ribosomes of all sizes and its properties are obscured.

Recently another type of RNA has been postulated, "Messenger RNA" (Jacob and Monod, 1961). This material is presumed to have a nucleotide composition similar to that of DNA and to have a high rate of turnover, being used to carry information from DNA to the site of protein synthesis and then being degraded to nucleotide. Evidence for the existence of RNA having complementarity to DNA has been found by Hall and Spiegelman (1961) who showed that hybrid molecules could be formed between some RNA and its related DNA.

Other studies (Gros *et al.*, 1961) directed towards the detection of messenger RNA have reported the presence of an RNA fraction which is rapidly labeled. However the properties of this fraction are indistinguishable from the properties of the ribosome presursor. Thus the question arises whether in addition there is a small fraction of rapidly turning over RNA which has a nucleotide sequence complementary to DNA, or whether the ribosome precursor may itself carry out the function of the postulated messenger.

In this and a following paper we present the results of studies of the incorporation of P^{32} and C^{14}-uracil into the RNA portion of ribosomes and the incorporation of C^{14}-amino acids into the protein portion. In addition ways of distinguishing ribosome precursor from messenger RNA are discussed.

B. MATERIALS AND METHODS

1. *Growth of Cells.* *E. coli* ML 30 was grown at 37° in C medium (Roberts *et al.*, 1955) with maltose as carbon source. An overnight culture was diluted with fresh medium and growth followed by optical density measurements at 650 mμ, for two or three generations of exponential growth so that an accurate estimate of the growth rate could be made under steady-state conditions. The generation time did not vary significantly from 51 minutes in any of these experiments.

Kinetic experiments began with the addition of the tracer. Measurements of the uptake of tracer into macromolecules (Paper I) and the increase in optical density were continued throughout the experiment.

In many experiments it proved convenient to use tracer methods for the measurement of total RNA as well as newly synthesized RNA. In these cases cells were grown for about three generations in C medium containing 1 to 2 mc $P^{32}O_4^{\equiv}$ per liter so that at least 88 per cent of the RNA molecules were P^{32}-labeled. The steady-state P^{32}-labeling of the RNA amounting to 70,000 to 140,000 CPM per mg RNA was used as a sensitive and accurate measure of the total nucleic acid in fractions free of phospholipid.

2. *Estimation of Radioactivity.* The 2-C^{14}-uracil was obtained from the California Corporation for Biochemical Research and the New England Nuclear Corporation and had specific radioactivities in the range 4 to 10 mc/mM.

Radioactivity present in RNA was estimated by adding trichloroacetic acid (TCA) to 5 per cent and passing through a 1 inch millipore filter (Britten, Roberts, and French, 1955). The filter was air-dried at 60-70°C for half an hour and suspended upright in a vial containing 10 ml of a 2,5-diphenyl oxazole 4 gm/liter (PPO) and 1,4-bis-2-(5-phenyloxazolyl) benzene 100 mg/liter (POPOP) solution in toluene. The samples were counted in an automatic Packard tri-carb liquid scintillation counter. Simultaneous counting of P^{32} and C^{14} was achieved with the aid of the split channel setting. At 870 volts C^{14} was counted with 40 per cent efficiency in the 10 to 50 volt channel with P^{32} contamination of 5 per cent. P^{32} was counted in the 100 volt to infinity channel together with only 1 per cent of the C^{14} count. The magnitude of these corrections was sufficiently low and constant for them to be made reliably on a routine basis.

3. *Analysis of Cell Extracts.* Cell samples were taken at suitable times during kinetic experiments by pouring rapidly onto crushed frozen medium. The cells were washed three times with cold tris chloride buffer 10^{-2} M, pH 7.4 containing magnesium chloride at concentrations from 10^{-2} to 10^{-4} as specified. The cells were resuspended in 1 to 2 ml of buffer and an extract prepared by passing through the orifice of a French pressure cell at 10,000 to 15,000 psi. In many cases DNAase was added to the cells immediately prior to the preparation of an extract.

Analysis of the cell extract on the basis of the varying rates of sedimentation of the various components, "sedimentation analysis," was made by the sucrose gradient technique already described (Britten and Roberts, 1960) with modifications to obtain higher resolution. With the original technique, the lower limit of the load of cell extract was determined by the necessity to read the ultraviolet absorption of the fractions. This normally required grading a 0.2 ml sample on the top of the swinging bucket tube. The use of a steady-state P^{32} label for measurement of the quantity of RNA greatly improved the sensitivity and made possible the use of much smaller samples of cell extract. Small samples are most conveniently loaded on the sucrose gradient by means of a pipet. A 0.07 or 0.05 ml drop of the cell extract was placed on a silicone-treated microscope slide near another drop of equal volume of 4 per cent sucrose solution in a tris buffer

containing $MgCl_2$ at a concentration from 10^{-2} to 10^{-4} M. A 0.2 ml pipet having the tip drawn out and slightly bent was used to suck up first the cell extract sample and then the sucrose solution. Slight tipping of the pipet removed any sharp boundary which might have formed between the two solutions. The whole contents of the pipet was then allowed to run gently onto the top of a 4.8 ml linear sucrose gradient from 20 per cent to 5 per cent in the same buffer made in the normal manner. After centrifuging for an appropriate time the contents of the tube was dripped out into about fifty fractions.

After adding 2 ml of cold 5 per cent TCA and allowing to stand for 20 minutes the radioactivity present in macromolecules was collected by passing through a membrane filter.

The DEAE cellulose used for chromatography of cell extracts was obtained from the California Corporation for Biochemical Research (cellex D, 0.91 meq/gm). The material was suspended in tris buffer 0.01 M containing $MgCl_2$ 0.01 M and brought to pH 7.4 with HCl. After the coarse fraction settled, the fine material was decanted with the supernatant. Three such washes were given. Columns of about 15 cm were packed in 1 cm tubes under 3 psi pressure. The samples of cell extract or ribosomes analyzed contained a maximum of about 5 mg RNA.

Elution was carried out with a linear sodium chloride gradient from zero to 1.0 M or from 0.2 M to 1.2 M in tris buffer 0.01 M, pH 7.4 containing $MgCl_2$ 0.01 M. The salt gradient was about 0.004 M/ml and the flow rate about 0.5 ml/min. About fifty fractions of 3.5 to 4.0 ml were collected.

4. *Extraction of RNA.* Duponol at 0.5 per cent was added to the total cell extract. This treatment dissociates the RNA from the protein (Kurland, 1960). Ribonuclease activity was prevented by the addition of 0.5 per cent duponol to the sucrose solutions in tris-HCl 0.01 M pH 7.4 used in sedimentation analysis.

C. RESOLUTION OF NUCLEOPROTEIN ON DEAE-CELLULOSE

Chromatography of a total cell extract on DEAE cellulose provides a useful method of separating ribosomes from the bulk of soluble cellular protein. While most of the soluble protein is eluted between zero and 0.3 M NaCl, ribosomes give a single peak at 0.4 M. Behind this ribosome peak, S-RNA elutes at 0.5 M and DNA at 0.6 M. Chromatography of P^{32} pulse-labeled extracts on DEAE shows the radioactivity in a region resolved from the main bulk of the ribosomes close to those of S-RNA and DNA. (Roberts *et al.*, 1958). At later times this radioactivity moves into the main nucleoprotein peak. These analyses suggested the existence of two sequential precursors in the synthesis of the RNA of the main nucleoprotein peak and that the resolution was a result of the lower protein content of the precursors. Detailed kinetic analysis of the results was not attempted due to the delay of the entry of the P^{32} radioactivity used as tracer into RNA by the large pool of nucleotide precursors. In contrast the special features of the entry of C^{14}-uracil into RNA already discussed (Paper I), giving an essentially linear curve of incorporation from time zero, make it much more suitable.

In Fig. 1 the DEAE chromatographic profiles are shown for four samples of a total cell extract taken 10, 20, 40, and 55 minutes after the addition of C^{14}-uracil.

The 0.4 M peak contains most of the ribonucleoprotein and the 0.5 to 0.6 M region S-RNA and the precursors. Even at 10 minutes it is evident that the precursor region has a specific radioactivity three to five times that of the main peak. Between 10 and 20 minutes the specific radioactivity of the main peak rises by more than a factor of three, demonstrating directly the existence of a sizeable precursor pool preceding it (Paper II).

A second experiment in which shorter exposures to C^{14}-uracil were employed

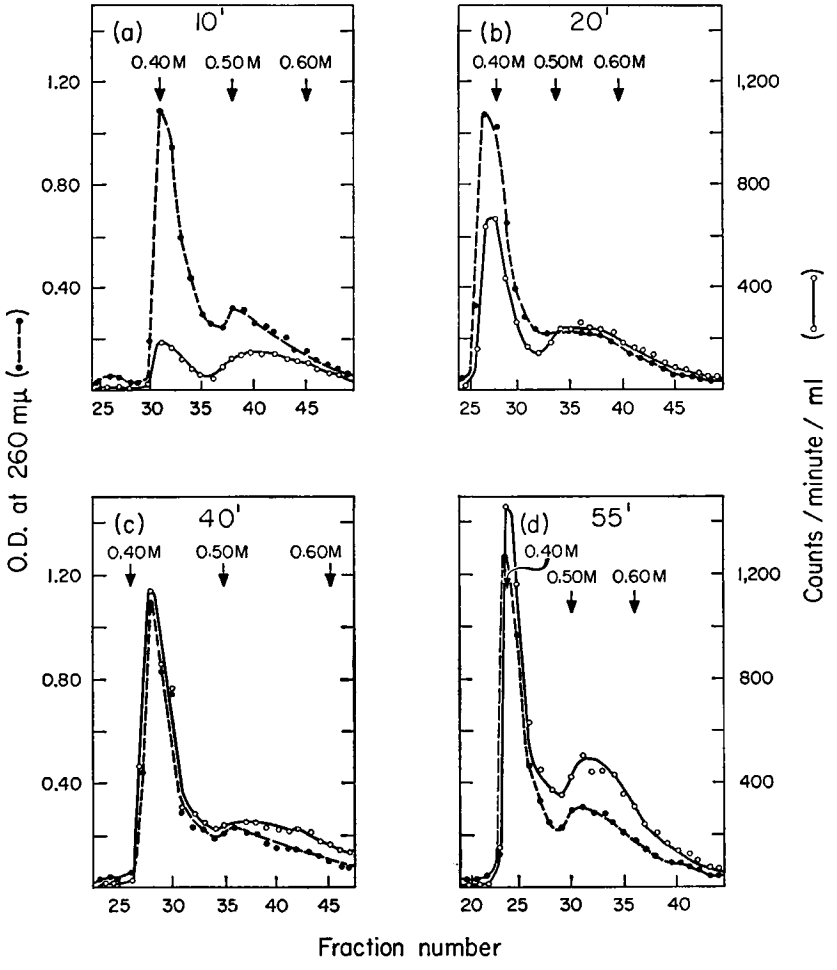

FIGURE 1 Analysis of total cell extracts on a DEAE-cellulose column. Linear sodium chloride gradient from zero to 1.0 M tris-HCl buffer 0.01 M, containing $MgCl_2$ 0.01M, pH 7.4, salt gradient 0.004 M/ml. Only the region in which RNA appears is plotted. The volumes collected varied between the four analyses but salt concentrations are indicated on each. The main peak includes most of the ribosomal material. S-RNA peaks at 0.5 M. (*a*) 10 minute exposure to C^{14}-uracil, (*b*) 20 minute, (*c*) 40 minute, (*d*) 55 minute.

proved to be more suitable for the separation of the three stages of ribosome synthesis and for the elucidation of their quantities and the flows through them. Six samples of cells were taken from a culture given from 25 second to 12 minute exposure to C^{14}-uracil. The cell extracts in tris buffer 10^{-2} M Mg^{++} were centrifuged for 4 hours at 40,000 RPM. The pellet contained essentially all of the ribosomal material and very little S-RNA. Chromatography of this pellet eliminated contamination of the ribosome precursor region around 0.5 M salt by S-RNA (Fig. 2).

The sequence of ribosome synthesis is readily observed in the six parts of Fig. 2. At 25 seconds, Fig. 2(*a*), all the radioactivity appears in a single peak at 0.6 M salt.

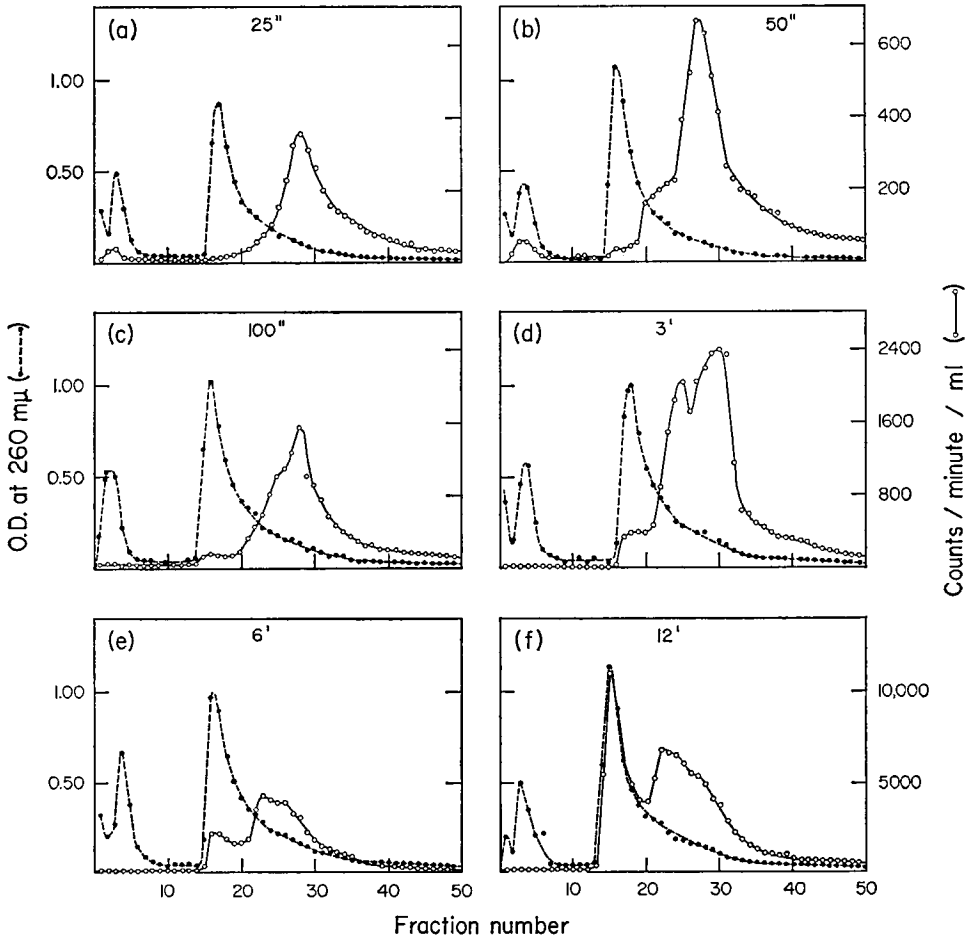

FIGURE 2 Analysis of total ribosomal pellets (40K 240 minute pellets) on a DEAE-cellulose column. Linear sodium chloride gradient from 0.2 M to 1.2 M in tris-HCl buffer 0.01 M containing $MgCl_2$ 0.01 M, pH 7.4. Salt gradient 0.004 M/ml. Volumes collected 3.6—3.8 ml. (*a*) 25 second exposure to C^{14}-uracil, (*b*) 50 second, (*c*) 100 second, (*d*) 3 minute, (*e*) 6 minute, (*f*) 12 minute.

At 50 seconds, Fig. 2(*b*), and 100 seconds, Fig. 2(*c*), a shoulder develops on the forward edge of this peak at 0.5 M to become dominant at 6 minutes, Fig. 2(*e*). Meanwhile the radioactivity associated with the main peak remains at a very low level in the first three analyses, subsequently rising very rapidly from 3 minutes to 12 minutes as shown in Fig. 2(*d*), (*e*), and (*f*).

For purposes of clarity and ease of discussion two sequential precursors in ribosome synthesis have been named eosome and neosome in order of synthesis. As will be shown later, these definitions do not rest only upon the distinctive chroma-

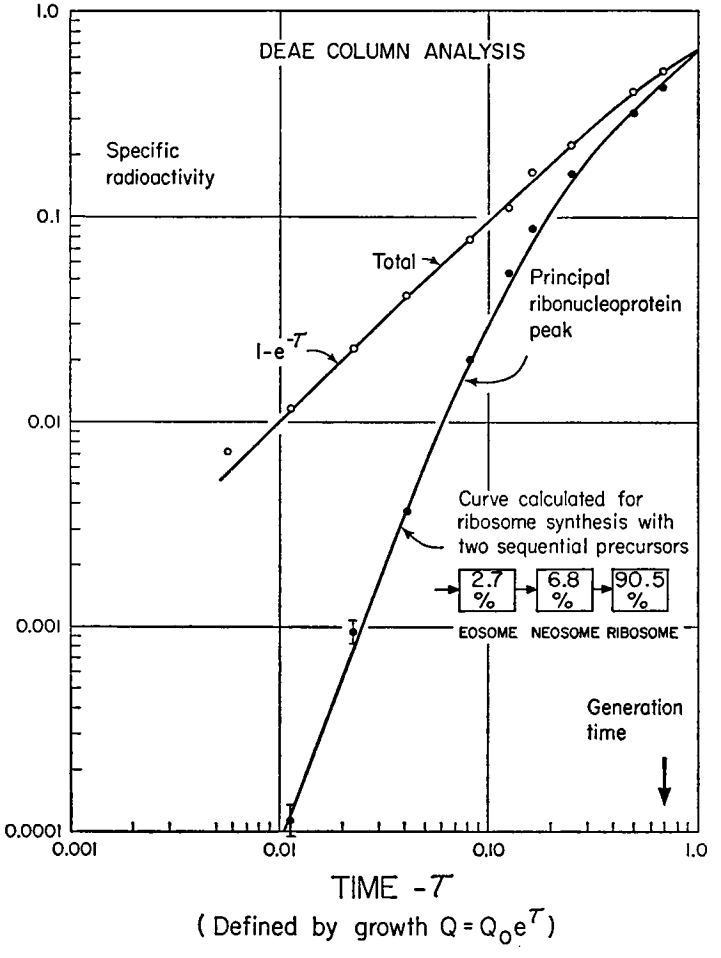

FIGURE 3 Log-log plot of the time course of specific radioactivity of the ribosome peak in a DEAE-cellulose column analysis. Time τ defined by $Q = Q_0 e^{\tau}$. Data from Fig. 1 and 2. The open circles represent the specific radioactivity of the total material eluted from the column Σ C^{14} / Σ O.D., 260mμ. The curve drawn through them is $1 - e^{-\tau}$. The curve drawn through the solid circles representing ribosome specific radioactivity was calculated for the example indicated on the figure.

tographic behavior, for the eosome and neosome can also be resolved from the bulk ribosomal material on the basis of their sedimentation coefficients.

The detailed analysis of the distribution of radioactivity between the ribosome peak and the two precursor stages was made in the following way.

1. The sample times were converted to τ with the knowledge of the generation time, *i.e.*, $\tau = t \log_e 2$ /generation time.

2. The total uracil label and the ultraviolet absorption at 260 mμ were summed for each column analysis and the ratio Σ C^{14} /Σ O.D. 260 mμ plotted against τ. Since this curve should fall on $\mu(1 - e^{-\tau})$, the factor μ was evaluated by sliding the points on the ordinate alone for a good fit (Fig. 3). The constant μ is a measure of the radioactivity per unit ultraviolet absorption of RNA at late times when $1 - e^{-\tau}$ approaches 1. It includes the specific radioactivity of the tracer and factors for the rate of utilization for RNA synthesis and the conversion to cytosine. The function is now $\phi_T = 1 - e^{-\tau}$ (Paper II). Since different concentrations and specific radioactivities of tracer were used μ was evaluated separately for the experiments of Figs. 1 and 2. Further, the slow rise in the rate of incorporation of uracil into RNA has been compensated in this way since the concentrations and time range of the two experiments were properly chosen.

3. The most easily calculated quantity is the specific radioactivity of the main ribosome peak μ_R/μ. Since it is the major component μ_R/μ is almost the same as ϕ_R. In this case it is in fact $1.1\phi_R$. No serious contamination of the first three or four fractions of this peak results from the radioactivity of percursor materials except in Figs. 2(*a*) and (*b*). No significant quantity of radioactivity can be attributed to the main ribosome peak in 2(*a*) and some correction for contamination was required for 2(*b*). The specific radioactivity is plotted against τ in Fig. 3. The magnitude of the depression of the ribosome specific radioactivity at early times is immediately diagnostic of two successive precursors since no one precursor could possibly be large enough to cause such a delay. The dependence of the specific radioactivity upon τ^3 at early times is also symptomatic of a delay by two precursors (Paper II). Fig. 3 also shows a theoretical curve drawn through the points, the justification for which will be given in a later paragraph.

4. A plot of ϕ_R *versus* Δ mass shows the delay of the entry of label into ribosomes due to the precursors. The intercept on the ordinate is a measure of the total quantity of precursor. This is true whether the precursors are sequential or parallel. Application of this procedure leads to a value of 9.5 per cent of the total ribosomal RNA as precursor.

5. Since the above determination indicates that the total quantity of precursor is much less than the total ultraviolet absorption in the region, it appears that most can be attributed to a streak of the main ribosomal peak. This can also be shown by chase experiments which fail to reduce the radioactivity in the region. Therefore, to a first approximation the radioactivity in the total precursor may be obtained by

subtracting the radioactivity due to the product ribosomal material at the specific radioactivity of the product peak. This is in fact a small correction except at very late times (Fig. 1). The total radioactivity in the precursor was then used to calculate ϕ_{N+E} which is plotted in Fig. 4.

6. Although it is apparent from the curves of Fig. 2 that there exist two components in the precursor region, the precision of any apportionment which can be made of the radioactivity between these two components is limited by the poor resolution. However from the earliest time point (25 seconds, Fig. 2(*a*)) a reason-

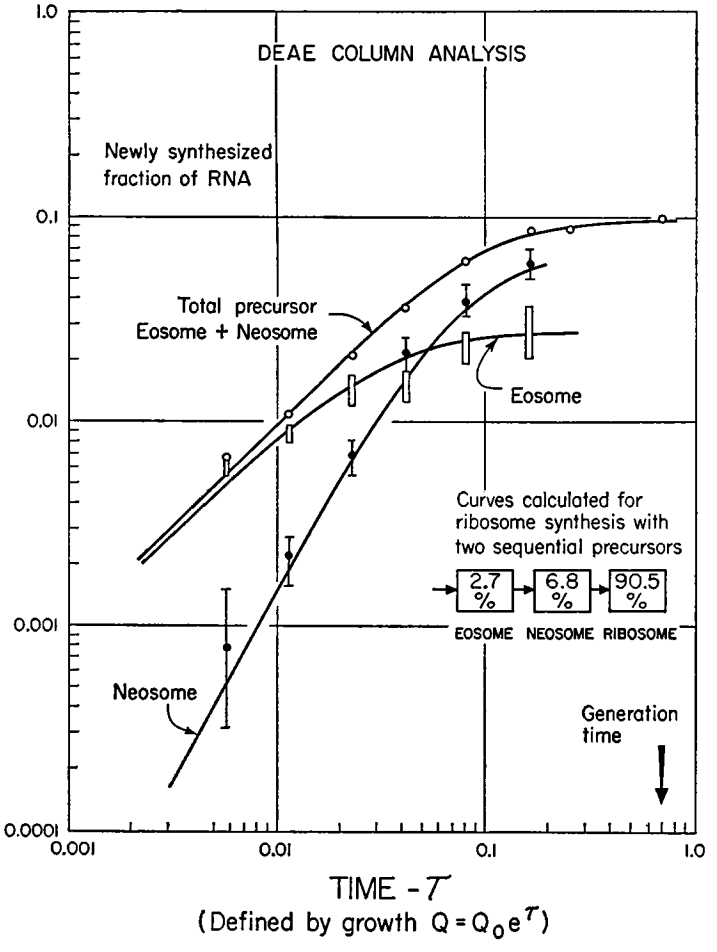

FIGURE 4 Log-log plot of the fraction of newly synthesized RNA present in total precursor and in eosome and neosome as a function of time. Data from Fig. 2 (two points from Fig. 1 at late times). The open circles represent total precursor, eosome plus neosome; the solid circles, neosome, and the bars eosome. The vertical lines are estimated ranges of possible error in the peak shape analysis. The three curves drawn are theoretical ones calculated for the example indicated on the figure.

able estimate of the peak shape of the eosome component may be made. Likewise, the peak shape of the neosome may be recognized from later points (Fig. 2(*f*)). The peak fractions of each of the components were located from the earliest and latest time points. The cross-contamination in each of these fractions by material of the other component was determined from the known peak shapes. Application of these corrections led to estimates of the fraction of the total precursor radioactivity attributable to each component. It was then possible to divide ϕ_{N+E} into ϕ_N and ϕ_E (Fig. 4).

7. To check the above procedure, numerical tables were made of functions for the peak shapes of the two precursor components. A least squares procedure was then applied to each time point for the separation into the two components. Agreement within the limits of precision was obtained between determinations made by the two procedures. In fact the evaluation of ϕ_N at very early times and ϕ_E at very late times, when each is a small fraction of the total precursor, is subject to considerable uncertainty due to the magnitude of the cross-contamination.

The results of these analyses are summarized in Figs. 3 and 4. The curve for μ_R/μ in Fig. 3 has a slope proportional to τ^3 at early times. Similarly the ϕ_N and ϕ_E curves of Fig. 4 have initial slopes proportional to τ^2 and τ. These relationships are direct indications of the sequence eosome → neosome → ribosome. The values at which the plots of ϕ_N and ϕ_E level off are direct measures of the quantities of each of the two precursors (Paper II). Of the total 10 per cent or so precursor material in ribosomal RNA about 2.5 per cent can be ascribed to eosomal material, and about 7 per cent to neosomal material. Theoretical curves for $\phi_N + \phi_E$ and μ_R/μ were calculated and fitted to the data in Figs. 3 and 4. The best fits were obtained using 2.7 per cent eosome, 6.8 per cent neosome, and 90.5 per cent ribosome.

D. INITIAL STUDIES BY MEANS OF SEDIMENTATION ANALYSIS

Most studies of the kinetics of ribosome synthesis have been carried out by means of sedimentation analysis in a magnesium concentration of 10^{-2} M necessary for the preservation of ribosomes. The general features of such analyses made on extracts from cells given a short pulse of either P^{32} or S^{35} have already been described (Roberts *et al.*, 1959; Roberts, 1960). At early times the specific radioactivities of the 30S and 50S ribosomes, present in the extract, were considerably higher than that of the 70S. These small particles, described as native 30S and 50S to differentiate them from those derived by breakdown of the 70S at lower magnesium concentrations, represent together some 10 to 20 per cent of the ribosomal material. Their higher specific activity after a pulse was interpreted as showing a precursor relationship to the 70S ribosomes.

Fig. 5 shows the analysis of extracts of four samples of cells taken after 10, 20, 40, and 55 minutes' exposure to C^{14}-uracil. 50S and 30S ribosomes show as shoul-

ders in the ultraviolet profile. At 10 minutes the specific radioactivities of the 50S and 30S ribosomes are at least three times that of the 70S. This difference in specific radioactivity decreases with time and has practically disappeared by 55 minutes. This long time uracil-labeling experiment appears to demonstrate qualitatively a precursor-product relationship between the native 50 and 30S and the 70S ribosomes.

When a series of cell extracts were prepared after much shorter exposures to C^{14}-

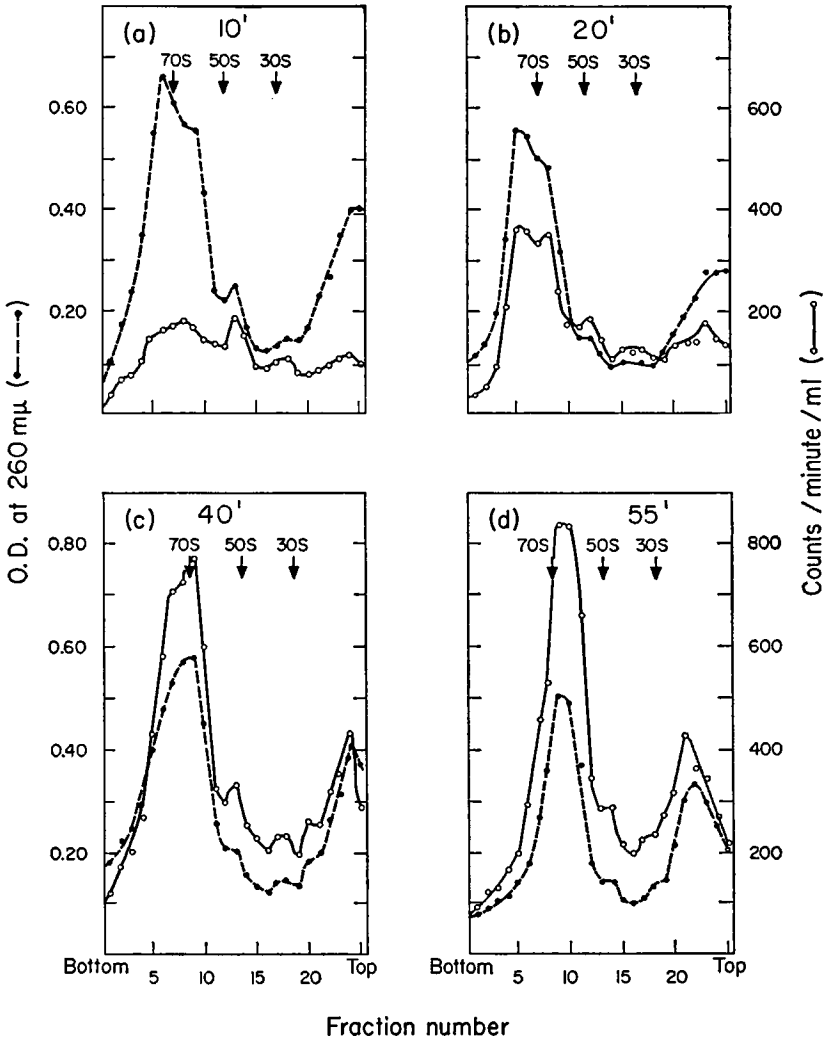

FIGURE 5 Sedimentation analysis of four total cell extracts taken from cells given (*a*) 10 minute, (*b*) 20 minute, (*c*) 40 minute, (*d*) 55 minute exposures to C^{14}-uracil. Centrifugation 90 minutes at 37,000 RPM. Cell washing, breakage, and centrifugation carried out in tris-HCl 0.01 M, pH 7.4, $MgCl_2$ 0.01 M.

uracil and analyzed in the same way (Fig. 6) the results were not interpretable on such a simple hypothesis. In this series of analyses the 50S and 30S ribosomes have a high specific radioactivity compared with that of the 70S although the ratio of specific radioactivities does not change greatly with time. In fact a simple precursor-product relationship would predict that the ratio be very large at early times if it is of the order of 3.0 at 12 minutes, as Figs. 5(*a*) and 6(*f*) show. This is evidently not the case and it appears that another process is dominant at early times causing radioactivity to appear in the 70S. This suggested direct entry of RNA into 70S

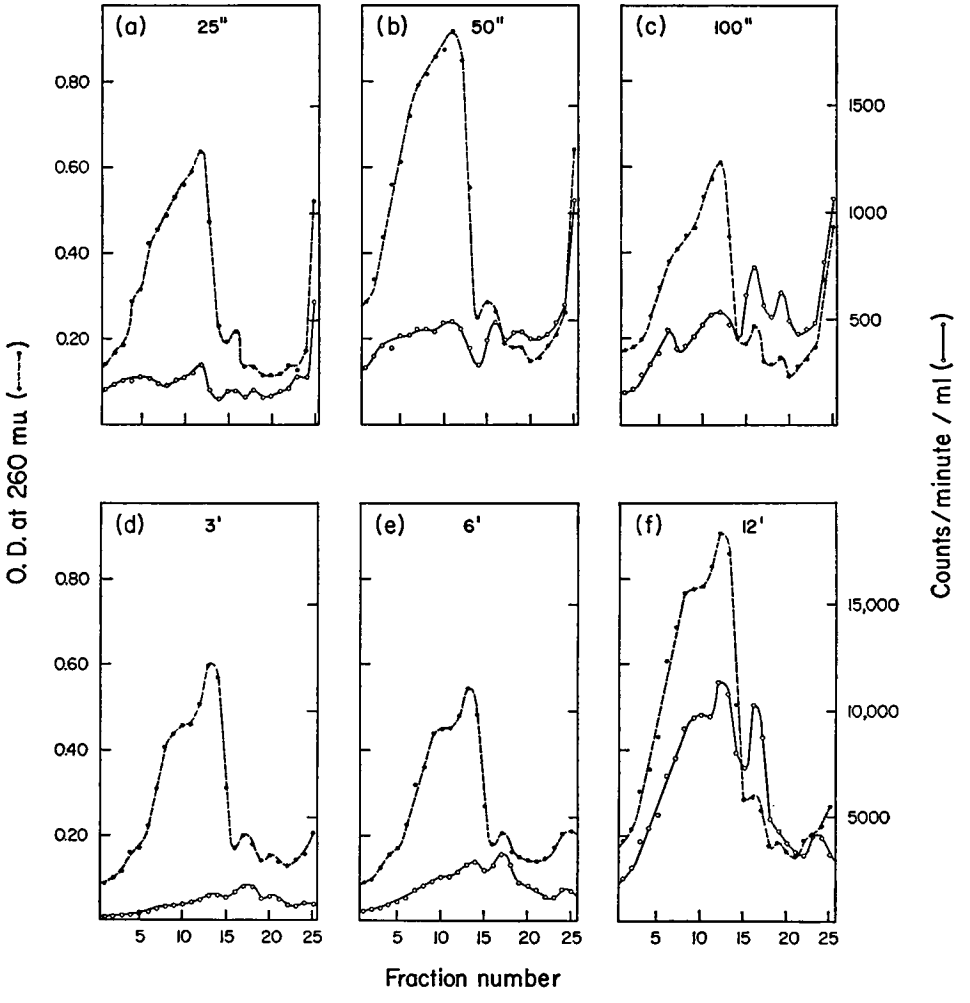

FIGURE 6 Sedimentation analysis of six total extracts taken from cells given (*a*) 25 second, (*b*) 50 second, (*c*) 100 second, (*d*) 3 minute, (*e*) 6 minute, (*f*) 12 minute exposures to C^{14}-uracil. Centrifugation 90 minutes at 37,000 RPM, 4°C. Cell washing and breakage centrifugation carried out in tris-HCl 0.01 M, pH 7.4, $MgCl_2$ 0.01 M.

without the delay brought about by passing through the large pools of 50S and 30S precursors. Another possibility was that this radioactivity was associated with the 70S peak rather than being incorporated into the large ribosomes. The increasing specific radioactivity towards the front edge of the 70S peak in Figs. 6(*a*) and (*b*) could be a result of the larger size of newly made particles or an increased quantity of radioactive material making some particles sediment more rapidly.

The next experiment was directed at selecting out the 70S ribosomes from a pulse-labeled extract and breaking them down to their constituent 50S and 30S

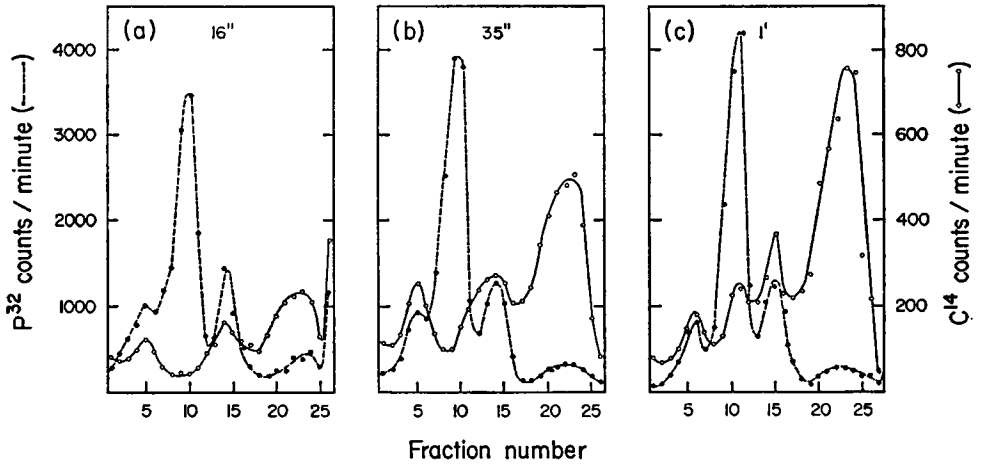

FIGURE 7 Sedimentation analysis of three 70S ribosome pellets purified by three successive 40K 30 minute centrifugations followed by a four hour dialysis against tris-HCl pH 7.4, 10^{-4} M $MgCl_2$. Cells pregrown for three generations in the presence of $P^{32}O_4\equiv$; thus the P^{32} radioactivity (dashed line) measures the total RNA of the ribosomes. C^{14}-uracil supplied for 16 seconds (*a*), 35 seconds (*b*), and 1 minute (*c*). Centrifugation 95 minutes at 37,000 RPM at 4°C in tris-HCl 0.01 M, pH 7.4, 10^{-4} M $MgCl_2$.

moieties so as to determine the location of this early radioactivity. Three samples of P^{32} steady-state labeled cells were taken after 16 seconds, 35 seconds, and one minute exposures to C^{14}-uracil, and extracts were prepared in tris HCl 0.01 M, pH 7.6, $MgCl_2$ 0.01 M. The cell walls and unbroken cells were removed by means of a five minute centrifugation at 40,000 RPM. The 70S ribosomes were selected from the supernatant by means of a thirty minute spin at 40,000 RPM and purified by two resuspensions and similar centrifugations. The final pellet, consisting largely of 70S ribosomes, contained 40 to 50 per cent of the total uracil radioactivity incorporated into RNA. The three pellets were resuspended and dialyzed against a large volume of tris HCl 0.01 M buffer containing $MgCl_2$ at 10^{-4} M for four hours. Sedimentation analysis on a sucrose gradient in 10^{-4} M magnesium produced the profiles of P^{32} and C^{14} radioactivity shown in Fig. 7. At least 90 per cent of the 70S

ribosomes have broken down into subunits of sedimentation coefficient approximately 50S and 30S. The customary 2/1 ratio in quantity of the subunits is not observed.

The distribution of C^{14} radioactivity shows that most of the pulse-labeled RNA now appears in a peak of low S number. At 16 seconds 50S ribosomes are virtually unlabeled compared with 30S ribosomes although about 20 per cent of the C^{14} remains associated with a peak of what are apparently residual 70S ribosomes. While the C^{14} radioactivity in the 30S ribosomes and in the 14S peak increase with time in Fig. 7(*b*) and (*c*), the small 70S peak becomes saturated very early with an apparent time constant of about 20 seconds. The quantity of uracil radioactivity in this component is about equal to that incorporated into total RNA during 2 seconds under the conditions of this experiment. Gros *et al.* (1961) have also observed this special component and estimate that it contains about 10 per cent of a 20 second pulse label. Thus it appears that the early label associated with the 70S ribosomes is of at least two types. The majority does not remain with the 50S and 30S after dissociation but appears in a peak of about 14S. Another rapidly saturating component remains associated with or is part of the few remaining large ribosomes having a sedimentation constant of about 70S.

Because of the complexity of analysis of cell extracts made in 10^{-2} M Mg^{++}, a search was made for conditions more suitable for the resolution of precursors from products in ribosome synthesis. Samples of cells were prepared having a steady-state P^{32} label and a 2 minute uracil pulse label. They were washed once in tris buffer containing 10^{-2} M Mg^{++} and then divided into four parts. The four samples were washed three more times in tris buffer containing magnesium chloride at 10^{-2} M, 3×10^{-3} M, 10^{-3} M, and 10^{-4} M, respectively, and finally resuspended and broken in the usual manner. All were analyzed on a sucrose gradient containing the appropriate magnesium concentration and the results are shown in Fig. 8. The first three samples were centrifuged at 37,000 RPM for 90 minutes and the last one for 150 minutes.

At 10^{-2} M Mg^{++} (Fig. 8(*a*)) most of the ribosomes are present as 70S but most of the radioactivity runs as 50S and 30S. The apparent specific radioactivity of the small ribosomes is greater than three times that of the 70S. Another feature worth noting is the higher specific radioactivity encountered on the leading edge of the 70S peak. Cells broken in the presence of 3×10^{-3} M Mg^{++} (Fig. 8(*b*)) have most of their ribosomes as 50S and 30S. At the same time about half of the radioactivity associated with ribosomes in Fig. 8(*a*) now appears in a peak of about 14S. There is now little difference between the specific radioactivities of the three groups of ribosomes although there is a peak of radioactivity running between the main 50S and 30S peaks. In 10^{-3} M magnesium (Fig. 8(*c*)), an even higher proportion of the radioactivity appears in a 14S peak, and the faster of the other two peaks of radioactivity appears to lag behind the 50S ribosome peak. The distribution of

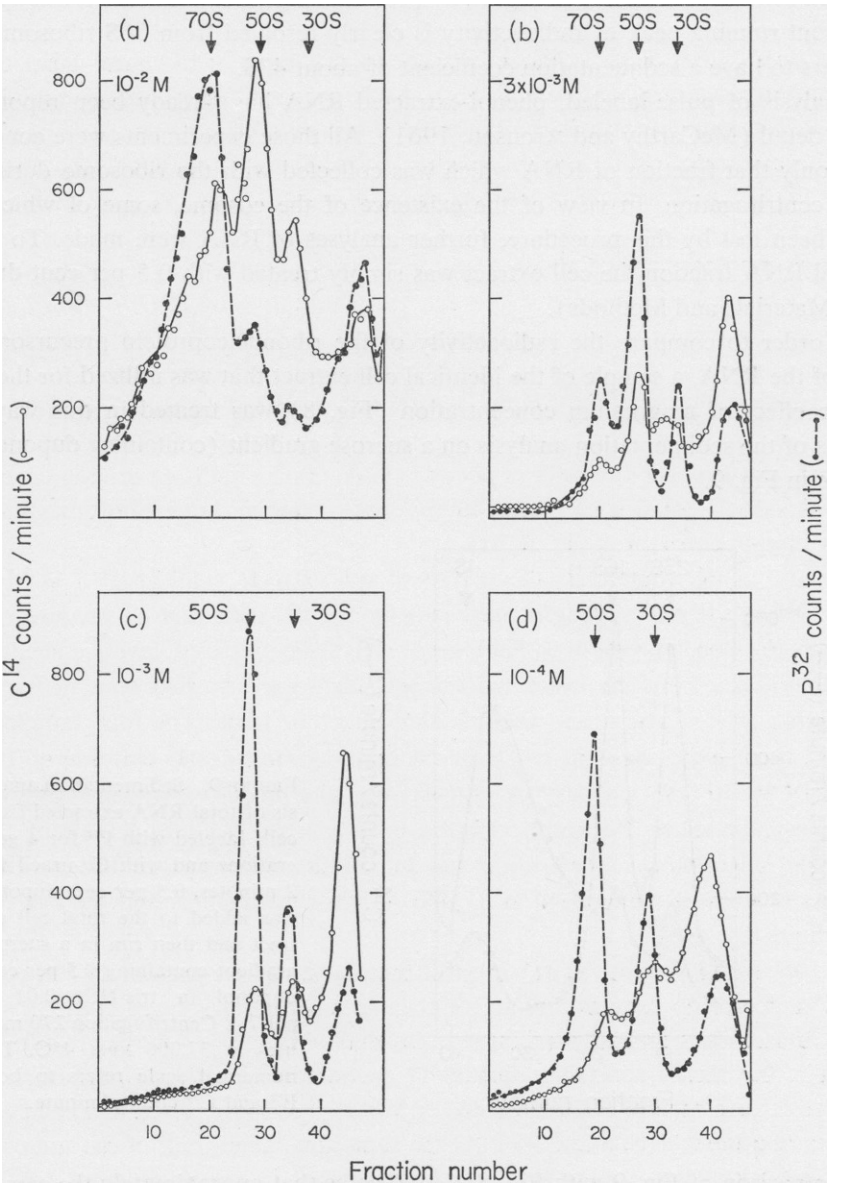

FIGURE 8 Sedimentation analysis of a total extract from cells labeled with P^{32} for four generations and with C^{14}-uracil for 2 minutes. Cells washed and extracts prepared and run in tris-HCl 0.01 M pH 7.4 containing $MgCl_2$ at (*a*) 10^{-2} M, (*b*) 3×10^{-3} M, (*c*) 10^{-3} M, (*d*) 10^{-4} M. Centrifugation (*a*), (*b*), (*c*) 90 minutes at 37,000 RPM, (*d*) 150 minutes at 37,000 RPM, 4°C. The numerical scale refers to both P^{32} and C^{14} counts/minute. Samples analyzed correspond to 0.5 mg dry weight of cells.

radioactivity between the three objects is very similar at 10^{-4} M Mg^{++} but the increased centrifugation time in Fig. 8(*d*) produces higher resolution. In this instance the front-running peak of radioactivity is clearly resolved from 50S ribosomes and appears to have a sedimentation coefficient of about 43S.

Analysis of pulse-labeled, phenol-extracted RNA has already been reported in some detail (McCarthy and Aronson, 1961). All those experiments were concerned with only that fraction of RNA which was collected with the ribosome during a 4 hour centrifugation. In view of the existence of the eosome, some of which may have been lost by this procedure, further analyses of RNA were made. To obtain a total RNA fraction the cell extract was simply treated with 0.5 per cent duponol (see Materials and Methods).

In order to compare the radioactivity of the ribonucleoprotein precursors with that of the RNA, a sample of the identical cell extract that was utilized for the study of the effect of magnesium concentration (Fig. 8) was treated in this way. The results of the sedimentation analysis on a sucrose gradient (containing duponol) are shown in Fig. 9.

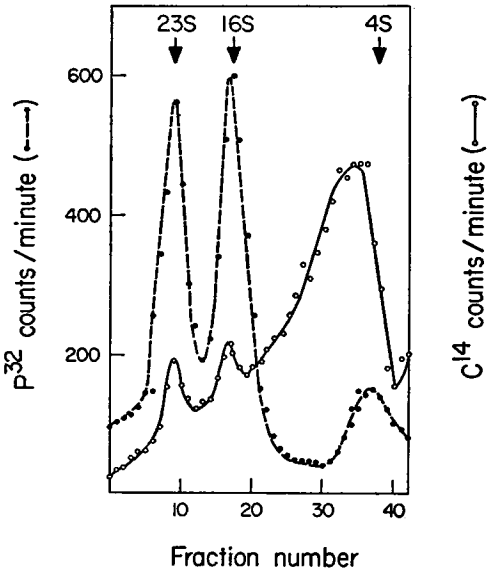

FIGURE 9 Sedimentation analysis of total RNA extracted from cells labeled with P^{32} for 4 generations and with C^{14}-uracil for 2 minutes. 0.5 per cent duponol was added to the total cell extract and then run in a sucrose gradient containing 0.5 per cent duponol in tris-HCl 0.01 M pH 7.4. Centrifugation 270 minutes at 37,000 RPM 4°C. The numerical scale refers to both P^{32} and C^{14} counts/minute.

Comparison of Fig. 9 with Fig. 8(*d*) indicates that approximately the same fraction of the RNA labeled for 2 minutes with uracil appears as complete 16S and 23S molecules, as that associated with the 30S and 43S peaks in the total extract. The rest of the C^{14} label appears in a peak of approximately 8S. Evidently the eosome appearing as 14S in the total extract appears as only 8S when treated with either duponol or phenol (McCarthy and Aronson, 1961; Gros *et al.*, 1961).

E. RESOLUTION OF THE RIBOSOME PRECURSORS BY SEDIMENTATION

The resolution of early labeled RNA from the bulk ribosomes suggested that these conditions of cell breakage and analysis of extracts would be suitable for the determination of the details of the kinetics of ribosome synthesis. At 2 minutes two objects other than the 50S and 30S ribosome peaks were highly labeled and readily resolvable. Further experiments were carried out to study their possible roles as ribosome precursors.

For this purpose careful analysis was made in 10^{-4} M magnesium of six samples of extracts prepared from P^{32} steady-state–labeled cells given from 30 seconds to 12

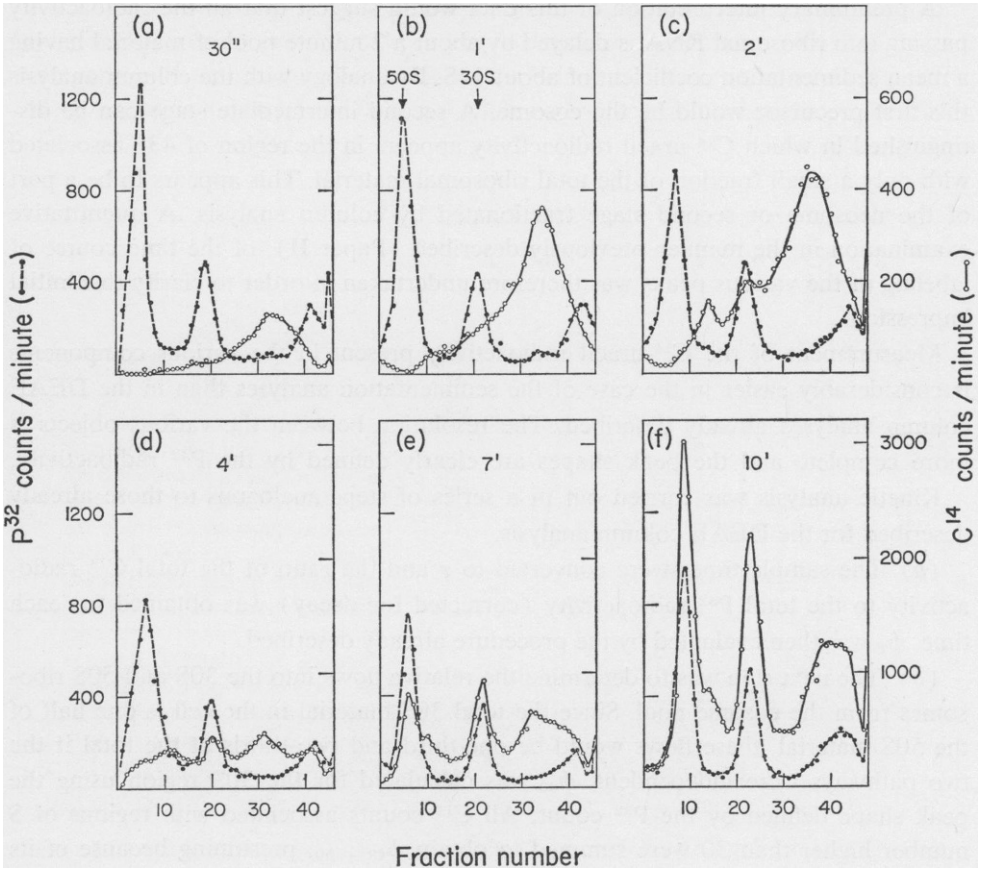

FIGURE 10 Sedimentation analysis of six DNAase-treated total extracts made and centrifuged in tris-HCl 0.01 M, pH 7.4 $MgCl_2$ 10^{-4} M from cells steady-state-labeled with P^{32} given (*a*) 30 second exposure to C^{14}-uracil, (*b*) 1 minute, (*c*) 2 minute, (*d*) 4 minute, (*e*) 7 minute, (*f*) 10 minute. Centrifugation 175 minutes at 37,000 RPM 4°C. Samples analyzed correspond to 0.5 mg dry weight of cells.

minutes exposure to C^{14}-uracil (Fig. 10). The extracts were treated with DNAase prior to centrifugation through a sucrose gradient. The P^{32} profile shows three main peaks of 50S and 30S ribosomes and soluble RNA. In Figs. 10(*a*) and (*b*) the C^{14} radioactivity appears almost entirely in the rather broad peak at about 14S. After 2 minutes there is little apparent rise in the specific radioactivity (C^{14}/P^{32} ratio) of this peak.

At 2 minutes two other peaks are clearly distinguishable; one associated with 30S ribosomes and another appearing between 30S and 50S at approximately 43S. The 43S component continues to rise in figures 10(*d*) and (*e*). Up to 7 minutes there is very little C^{14} radioactivity which can be associated with the 50S peak but then the radioactivity increases by a factor of about 10 between 4 minutes and 10 minutes.

A preliminary interpretation of this data would suggest that all the radioactivity passing into ribosomal RNA is delayed by about a 2 minute pool of material having a mean sedimentation coefficient of about 14S. By analogy with the column analysis this first precursor would be the eosome. A second intermediate stage can be distinguished in which C^{14}-uracil radioactivity appears in the region of 43S associated with only a small fraction of the total ribosomal material. This appears to be a part of the neosome or second stage fractionated by column analysis. A quantitative examination in the manner previously described (Paper II), of the time course of labeling of the various peaks was therefore undertaken in order to clarify this initial impression.

Measurement of the C^{14}-uracil radioactivity present in the various components is considerably easier in the case of the sedimentation analyses than in the DEAE column analyses already described. The resolution between the various objects is more complete and the peak shapes are clearly defined by the P^{32} radioactivity.

Kinetic analysis was carried out in a series of steps analogous to those already described for the DEAE column analysis.

(*a*) The sample times were converted to τ and the ratio of the total C^{14} radioactivity to the total P^{32} radioactivity (corrected for decay) was obtained for each time. ϕ_T was then evaluated by the procedure already described.

(*b*) The next step was to determine the relative flows into the 30S and 50S ribosomes from the eosome pool. Since the total 30S material in the cell is one half of the 50S material, these flows would be one-third and two-thirds of the total if the two pathways were independent. ϕ_{30} was calculated for the 30S region using the peak shape defined by the P^{32} count. All C^{14} counts associated with regions of S number higher than 30 were summed to obtain ϕ_{43+50}, presuming because of its sedimentation constant that the 43S peak was a precursor of the 50S. These two functions are plotted in Fig. 11. It is immediately clear that the curves are not a factor of two apart and especially at early times the 30S region has more than its share of radioactivity. It appears that a precursor of the 50S ribosome is present in the 30S region.

(*c*) In a more detailed analysis ϕ_E (eosome), ϕ_{43}, and ϕ_{50} were evaluated. At early times ϕ_{30} and ϕ_{43} are not known very precisely due to contamination by the trail of eosome. The peak shape of eosome, however, is such that reasonable estimates can be made. Further, ϕ_E cannot be estimated directly at late times but must be corrected for the growing radioactivity of S-RNA. In making this correction the quantity of S-RNA was evaluated from the P^{32} radioactivity in the region of small sedimentation coefficient. Its specific radioactivity was taken to be equal to that of the total RNA (ϕ_T), since there is no evidence for a delay in its labeling. In the case of the 43S reasonably precise estimates can be made out to 10 minutes due to the strong depression of ϕ_{50} and an accurate knowledge of the peak shape obtained from Fig. 10(*c*).

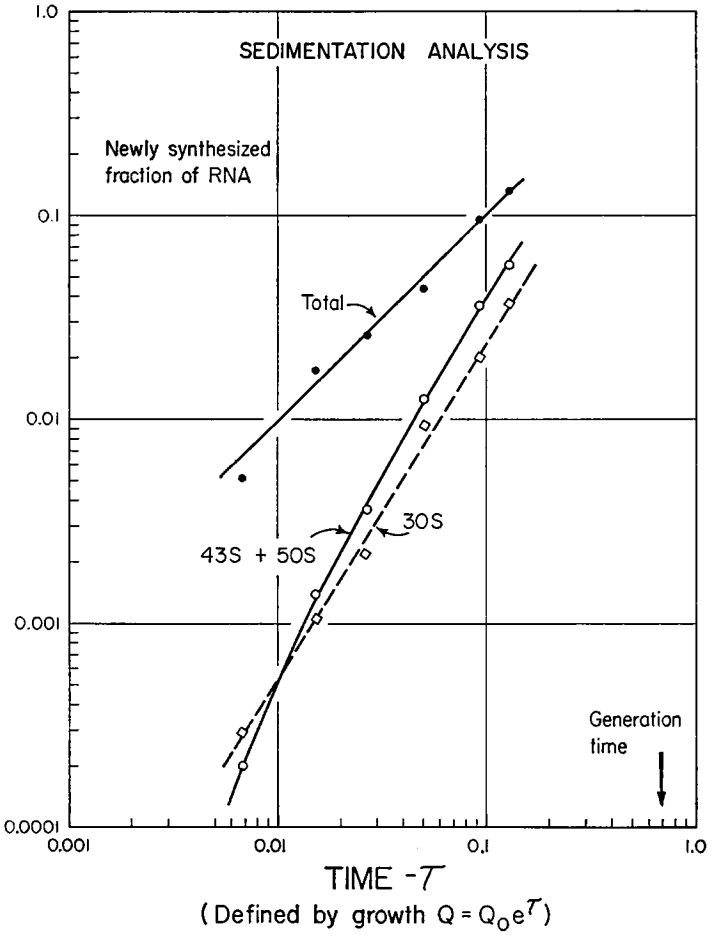

FIGURE 11 Log-log plot of the newly synthesized fraction of RNA present in total cell extract (•), 30S region (□), and 43S + 50S region (o) as a function of time. Data from Fig. 10.

(*d*) The three functions ϕ_E, ϕ_{43}, and ϕ_{50} are plotted together with ϕ_T in Fig. 12. The curve for ϕ_E is essentially the same as that obtained by column analysis (Fig. 4). The value at which it levels off indicates a pool size of about 2 per cent of the total ribosomal RNA for the eosome. Since the eosome accounts for the total flow at early times both ϕ_{43} and ϕ_{50} are strongly depressed at early times. ϕ_{43} is proportional to τ^2 at early times and ϕ_{50} to τ^3. This would be expected if the 43S component is the neosome or second stage in the synthesis of the 50S ribosome.

The objects first to receive radioactivity, variously called 14S RNA, eosome, informational RNA, or messenger RNA are probably of great importance to the

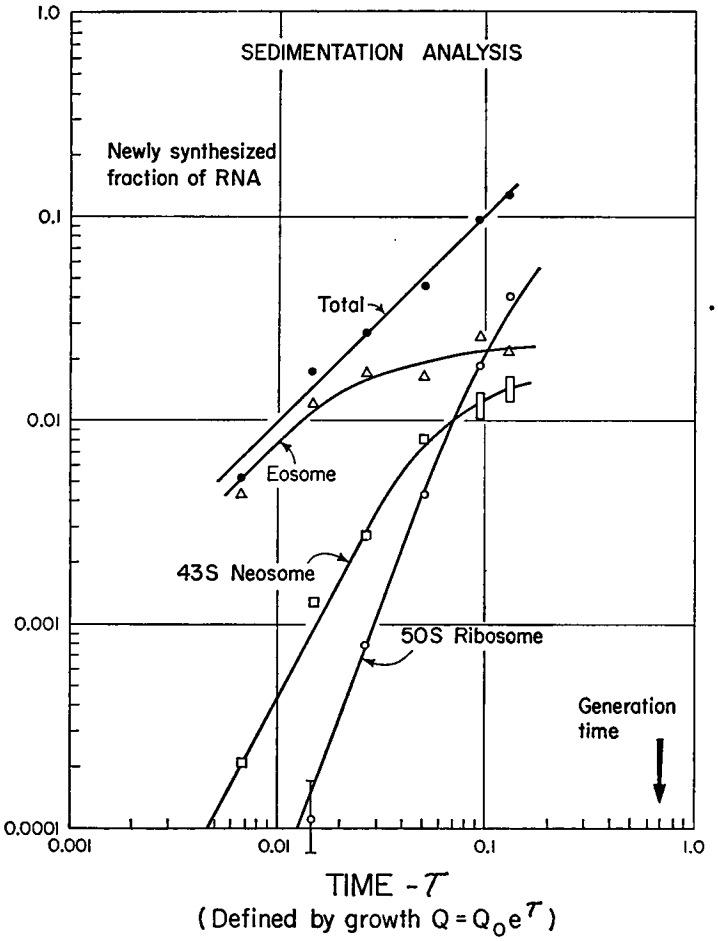

FIGURE 12 Log-log plot of the newly synthesized fraction of RNA present in the total cell extract (•), eosome (△), 43S neosome (□), and 50S ribosome (o) as a function of time. Data from Fig. 10. The curve drawn for the 50S ribosomes is the calculated curve shown on Fig. 3 multiplied by two-thirds since the 50S ribosomes account for two-thirds of the ribosomal nucleoprotein. The agreement is striking.

central problem of the origin and function of ribosomal RNA. Therefore the evidence showing that the RNA in the 14S region is precursor to ribosomal RNA will be examined in detail. For this purpose the more conventional linear plot of the time course of labeling, shown in Fig. 13 is a useful adjunct to the curves shown in Figs. 11 and 12.

On Fig. 13 are shown first the radioactivity in the total RNA, ϕ_T' (reduced by 15 per cent to correct for the soluble RNA), second the radioactivity of the 14S region, ϕ_E, corrected at late times for the soluble RNA, as described above, and third the radioactivity of neosome plus ribosome, $\phi_{30} + \phi_{43} + \phi_{50}$ called here ϕ_R'.

All of the radioactivity initially enters the eosome, thus at early times $\phi_T' = \phi_E$. Later ϕ_E levels off at 0.02 corresponding to 2 per cent of the total ribosomal RNA.

If the total flow to ribosomal RNA passed through an object of this size the time constant would be about 2 minutes which is consistent with the shape of the curve for ϕ_E.

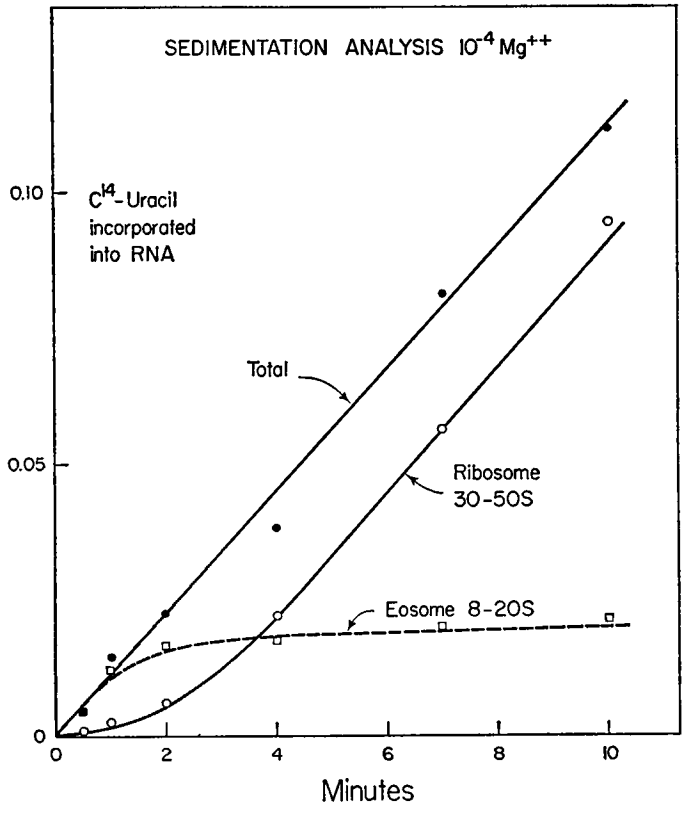

FIGURE 13 The C^{14}-uracil label incorporated into total RNA (•), the eosome region 8-20S (□), and the ribosome region (o), *i.e.*, material between 30S and 50S including neosome and ribosome. Data from Fig. 10. The label in each component is plotted as ϕ functions ϕ_T, ϕ_E, ϕ_{R+E} as in Figs. 11 and 12.

The curve for ϕ_R' has zero slope at zero time showing that the entry of radioactivity is delayed by a precursor. Further, the ribosome curve, ϕ_R' falls below ϕ_T' at late times by an amount equal to the quantity of the eosome. Thus the delay of ϕ_R' is approximately correct for the size of the eosome. While ϕ_R' rises initially in proportion to τ^2 the values at 30 seconds and 1 minute are lower than would be expected. Using the equation shown in Paper II, Fig. 1, for the earliest time points, the calculated quantity of precursor is 3.5 per cent of the total ribosomal RNA. This difference may be due to an underestimate of ϕ_{30} or may indicate that the quantity of eosome is somewhat greater than 2 per cent, as does the DEAE analysis. Alternatively, there may be a time required for completion of the eosome before it can be utilized for neosome synthesis. In any case it is clear that very little if any C^{14}-uracil radioactivity bypasses the eosome on its way to neosome or ribosome.

F. DISCUSSION

From the analysis of uracil-labeled cell extracts, it is clear that at early times all the radioactivity is present in a fraction, named eosome, peaking at 14S. The kinetic behavior of the component has been studied and its size estimated at 2 to 3 per cent of the total ribosomal RNA. It can be shown from the same experiments that label entering nucleoprotein of higher molecular weight is delayed by a component of about the same size. Together these observations suggest that the eosome is predominantly precursor to ribosomes.

In another recent study (Gros *et al.*, 1961) however, the rapidity of labeling of the eosome has been invoked as a criterion of turnover. These authors have suggested that the rapid rate with which label enters and leaves the eosome fraction proves instability of these RNA molecules. In general, however, it is clear that the rapid labeling of a small component indicates merely that the flow into it is much larger than that required to maintain its quantity in the growing cell. The loss of label when an excess of unlabeled isotope is added shows only the already obvious fact that there is also a transfer of material out of this component. These qualitative measurements cannot be expected to distinguish between a precursor through which label flows to a product and a compound which is synthesized and then is broken down to its constituent parts. To some extent, the lack of distinction between these two alternatives results from the use of the word turnover without properly stating the level of turnover that is being considered. In order to distinguish between the two very different alternatives it would be preferable if the term were reserved for phenomena of molecular instability since the word precursor is an adequate description of the other alternative.

The difficulty of demonstrating true turnover in the sense of synthesis and degradation of a given molecule has already been discussed (Paper I). What we have demonstrated is that there exists a precursor-product relationship between the eosome and the product ribosomes for the transfer of C^{14}-uracil radioactivity.

It does not prove conclusively that labeled molecules initially observed as eosomes are incorporated *as such* into completed ribosomes. An alternative involves breakdown of the eosome molecules and a synthesis of ribosomes by means of a quantitative reutilization of the labeled degradation products. It should be pointed out that in common with many similar tracer studies the latter alternative cannot be rigidly ruled out. In order to conserve the label for quantitative reutilization, the breakdown has to occur in such a way that there is no mixing with other unlabeled RNA precursors (Paper I). In the absence of evidence for such a breakdown of

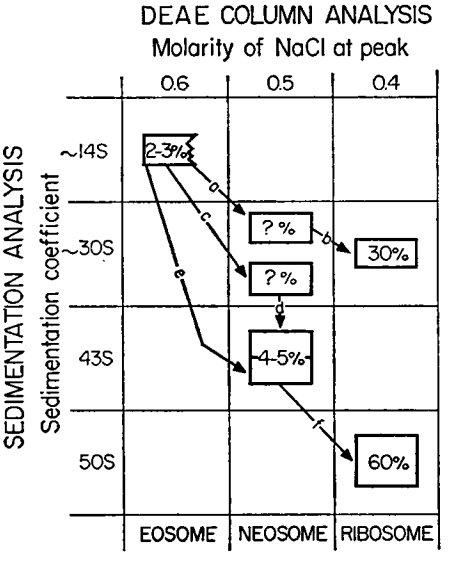

FIGURE 14 Schematic diagram of the flow of RNA in ribosomal synthesis. The diagram indicates the way in which the information derived from DEAE-cellulose column analysis and sedimentation analysis has been combined to give a more complete scheme. The figures in the boxes represent the percentages of the total ribosomal RNA existing in each of the states in a steadily growing cell. Movement downwards is a result, principally, of the completion of RNA subunits. Movement to the right is principally a result of the addition of protein.

eosome molecules, the data have been interpreted in terms of a precursor-product relationship.

As far as the details of ribosome synthesis are concerned it is clear that three main stages may be described. The clearest demonstration derives from the rate of labeling of the main ribonucleoprotein peak in the column analysis. Its radioactivity rises initially as the cube of time. The total label present at early times is so low as to require two sequential precursors. The total precursor material can be only 10 per cent of the total RNA and a single precursor of this magnitude could not introduce such a delay into the product (Paper II, Fig. 1).

Separation of the total precursor material into the two components is, in fact, achieved by the DEAE-cellulose chromatography. The primary eosome stage can be shown to be 2 to 3 per cent of the total ribosomal RNA and the second neosome stage 6 to 7 per cent. The time variation of the label entering the second peak shows it to be delayed by one precursor.

Sequential precursors are also clearly shown by sedimentation analysis. The 50S

peak is very well resolved from precursor material and shows the same time course of labeling as the main ribonucleoprotein peak in column analysis. As shown by a comparison of Fig. 3 and Fig. 12 the radioactivity of the 50S is just two-thirds of the main ribonucleoprotein peak as would be expected since the 50S ribosome makes up two-thirds of the 70S ribosome.

The diagram shown in Fig. 14 summarizes the results obtained with both types of analysis and indicates the correlation between the two. In the following paragraphs the evidence which supports each of the features of this diagram will be considered.

Eosome. The interpretation of the role of the eosome as precursor to all of the ribosomal RNA has been discussed above. It is not to be supposed that the eosome is one homogeneous class. It has a broad range of sedimentation constants and presumably supplies the RNA to a variety of ribosomes. In particular the nucleotide compositions of the 30S and 50S ribosomes differ (Bolton, 1959). The peak at 0.6 M in the column analysis and the broad region peaking at 14S in the sedimentation analysis both carry all of the radioactivity at early times and later saturate at about the same quantity of radioactivity.

Flows a and b and the 30S Neosome Precursor to 30S Ribosomes. It is clear from the column analysis that there exists a neosome precursor to 30S ribosomes since the peak eluted at 0.4 M contains both the 30S and 50S ribosomes, the radioactivity entering it is very strongly delayed and rises as τ^3 at early times. The only location in the sedimentation analysis (Fig. 10) where such an object can occur is in the 30S region. Because of the lack of resolution it has been impossible independently to assess its kinetics of labeling or measure its quantity. After correction for the trails of 43S and eosome peaks in Figs. 10(c) and (d), it appears that the C^{14} radioactivity in the 30S region reaches its maximum somewhat behind the P^{32} peak corresponding to the 30S ribosomes. This result is quite uncertain but leaves an impression of heterogeneity in the 30S region.

Flows c and d and the 30S Precursor to 50S Ribosomes. Fig. 11 shows that there is a greater flow into the 30S region than is required for the synthesis of the 30S ribosomes, in fact more than half the flow from the eosome passes into the 30S region at early times. This shows that a part of the flow that ultimately reaches the 50S ribosome passes through a 30S neosome. We have chosen to indicate on the diagram that one half of the flow to 50S passes this way for the following reasons. In the first place the 43S radioactivity (Fig. 12) is one-third of the neosome radioactivity (Fig. 4) at early times. In the second place a sedimentation coefficient of 30S suggests that one-half of the 50S RNA is already present. It is not clear whether the two 30S neosomes indicated are identical to each other. The nucleotide compositions of the 50S and 30S ribosomes differ but this difference could be made up through the flow e. The total quantity of the 30S neosomes can be crudely estimated by the difference between the amount of 43S neosome (4 to 5 per cent) and the total amount of neosome (7 per cent) indicated on Fig. 4. No estimate of

the relative quantities of the two objects indicated can be made if in fact they differ.

The 43S Neosome and Flows e and f. The 43S neosome stands out clearly in sedimentation analysis (Fig. 10(*c*)) at the appropriate time. The time course of labeling shown on Fig. 12 is that of the neosome or second stage in the sequence. The radioactivity rises as τ^2 initially and levels off later. At early times the curve has the shape of ϕ_N (Fig. 4) but only one-third of the magnitude of ϕ_N. If the total flow to the 50S ribosomes passed directly to the 43S from the eosome, ϕ_{43} would be expected to be just two-thirds of ϕ_N. Therefore it is clear that about half the flow to 50S ribosomes passes to the 43S from the eosome.

It appears certain that no eosomal RNA goes directly to the 50S ribosome because ϕ_{50} is proportional to τ^3 at early times. The 43S neosome is shown on the diagram as containing the full complement of RNA of the 50S ribosome. This seems likely from its sedimentation constant.

The quantity of 43S neosomal RNA can be estimated to be about 5 per cent from the steady-state P^{32} radioactivity that remains in this region after the 30S and 50S contributions have been subtracted, assuming reasonable and symmetrical peak shapes. The specific radioactivity estimated on this basis at early times is just one-half what would be expected if the total flow to 50S ribosomes passed directly from the neosome to the 43S. This is, of course, consistent with the diagram since one-half of the flow should be delayed by the 30S neosome precursor to the 43S.

The diagram (Fig. 14) shows a set of sequential relationships which are more complex than the two sequential precursors shown on Fig. 3. The diagram suggests that half of the radioactivity of the 50S ribosomes should rise in proportion to τ^4 for a time while the other half should rise as τ^8. All of the 30S ribosome radioactivity should rise as τ^3.

While deviations from the 3-stage model showed clearly in the time course of labeling precursors such as the 30S and 43S neosomes, the accuracy of the data is not adequate to resolve the predicted fourth power component in the final product.

These studies of the synthesis of the RNA portion of ribosomes provide only a few hints to the concurrent process of the addition of protein. The step from 43S neosome to 50S ribosome involves both a change in sedimentation coefficient and a change in the elution from DEAE, but no additional RNA is added. It seems quite obvious that this change is due to a change in the protein content. Studies using C^{14}-leucine to follow the synthesis of the protein are described in the following communication (Paper IV).

Received for publication, August 22, 1961.

REFERENCES

BOLTON, E. T., *Carnegie Institution of Washington Year Book No. 58*, 1959, 275.
BRITTEN, R. J. and ROBERTS, R. B., *Science*, 1960, **131**, 32.

BRITTEN, R. J., ROBERTS, R. B., and FRENCH, E. F., *Proc. Nat. Acad. Sc.*, 1955, **41**, 863.
GROS, F., HIATT, H., GILBERT, W., KURLAND, C. G., RISEBROUGH, R. W., and WATSON, J. D., *Nature*, 1961, **190**, 581.
HALL, B. D. and SPIEGELMAN, S., *Proc. Nat. Acad. Sc.*, 1961, **47**, 138.
JACOB, F., and MONOD, J., *J. Molecular Biol.*, 1961, **3**, 318.
KURLAND, C. G., *J. Molecular Biol.*, 1960, **2**, 83.
MCCARTHY, B. J., and ARONSON, A. I., *Biophysic. J.*, 1961, **1**, 227.
MCQUILLEN, K., ROBERTS, R. B., and BRITTEN, R. J., *Proc. Nat. Acad. Sc.*, 1959, **45**, 1437.
ROBERTS, R. B., *Ann. New York Acad. Sc.*, 1960, **88**, 752.
ROBERTS, R. B., ABELSON, P. H., COWIE, D. B., BOLTON, E. T., and BRITTEN, R. J., *Carnegie Institution of Washington Pub. No. 607*, 1955.
ROBERTS, R. B., ARONSON, A. I., BOLTON, E. T., BBITTEN, R. J., COWIE, D. B., MCCARTHY, B. J., MCQUILLEN, K., and DUERKSEN, J. D., *Carnegie Institution of Washington Year Book No. 59*, 1960, 229.
ROBERTS, R. B., BOLTON, E. T., BRITTEN, R. J., and COWIE, D. B., *Carnegie Institution of Washington Year Book No. 57*, 1958, 127.
ROBERTS, R. B., BOLTON, E. T., BRITTEN, R. J., COWIE, D. B., MCCARTHY, B. J., and MCQUILLEN, K., *Carnegie Institution of Washington Year Book No. 58*, 1959, 259.
ROBERTS, R. B., BRITTEN, R. J., and BOLTON, E. T., *in* Microsomal Particles and Protein Synthesis, (R. B. Roberts, editor), New York, Pergamon Press, 1958, 84.
TISSIÈRES, A., SCHLESSINGER, D., and GROS, F., *Proc. Nat. Acad. Sc.*, 1960, **46**, 1450.